University of Huddersfield Repository

Guan, Q, Yap, Y. F., Goharzadeh, A., Chai, John, Vargas, F. M., Chapman, W and Zhang, M.

Integrated One-Dimensional Modeling of Asphaltene Deposition in Wellbores/Pipelines

Original Citation

Guan, Q, Yap, Y. F., Goharzadeh, A., Chai, John, Vargas, F. M., Chapman, W and Zhang, M. (2017) Integrated One-Dimensional Modeling of Asphaltene Deposition in Wellbores/Pipelines. In: Seventh International Conference on Modeling, Simulation and Applied Optimization, April 4th-6th 2017, UAE. (Submitted)

This version is available at http://eprints.hud.ac.uk/id/eprint/30994/

Integrated One-Dimensional Modeling of Asphaltene Deposition in Wellbores/Pipelines

Q. Guan, Y.F. Yap*, A. Goharzadeh
Department of Mechanical Engineering
The Petroleum Institute
Abu Dhabi, UAE
*email: yfatt@pi.ac.ae

F.M. Vargas, W.G. Chapman
Department of Chemical and Biomolecular Engineering
Rice University
Houston, USA

J.C. Chai
Department of Engineering and Technology
University of Huddersfield
Huddersfield, UK

M. Zhang
School of Energy and Power Engineering
Nanjing University of Science and Technology
Nanjing, P.R. China

Abstract—*Asphaltene deposition in wellbores/pipelines causes serious production losses in the oil and gas industry. This work presents a numerical model to predict asphaltene deposition in wellbores/pipelines. This model consists of two modules: a Thermodynamic Module and a Transport Module. The Thermodynamic Module models asphaltene precipitation using the Peng-Robinson Equation of State with Peneloux volume translation (PR-Peneloux EOS). The Transport Module covers the modeling of fluid transport, asphaltene particle transport and asphaltene deposition. These modules are combined via a thermodynamic properties lookup-table generated by the Thermodynamic Module prior to simulation. In this work, the Transport Module and the Thermodynamic Module are first verified and validated separately. Then, the integrated model is applied to an oilfield case with asphaltene deposition problem where a reasonably accurate prediction of asphaltene deposit profile is achieved.*

Keywords—*integrated modeling, 1D, asphaltene deposition, wellbore/pipeline, thermodynamic module, transport module*

I. INTRODUCTION

Asphaltene deposition can appear at various stages of oil production, transportation and processing, leading to arterial blockages of wellbores, pipelines, separators, heat exchangers and other surface facilities [1-3]. As oil flows in wellbores or pipelines, due to the change in pressure (p), temperature (T) and oil composition, asphaltene precipitation usually takes place producing particles. Some of these particles deposit on wall surface forming an asphaltene deposit layer. The effective flow area is reduced and the pressure drop increases resulting in reduced oil production. The preventive and remedial measures are accompanied by economic losses in the form of treatment cost and daily production loss [4]. This necessitates improved methods to accurately forecast asphaltene deposition in wellbores or pipelines.

Ramirez-Jaramillo *et al.* [5] developed a multiphase multi-component hydrodynamic model for asphaltene deposition in production pipelines. Soulgani *et al.* [6] fitted a correlation for asphaltene deposition rate and coupled to the correlation of Begges and Brill [7] for flow with asphaltene precipitation determined the approach in [8]. Eskin *et al.* [9-10] developed an asphaltene deposition model in pipelines with shear removal included under the assumption that only the particles smaller than a critical size can deposit. Vargas *et al.* [11] proposed a model which simultaneously considered asphaltene precipitation, particle transport, asphaltene aggregation and deposition. Kurup *et al.* [12-13] further simplified the model to one-dimension, and included diffusion due to turbulent velocity fluctuation.

In these aforementioned studies, the coupling effect of the growing deposit layer on flow fields and eventually the deposition process itself has not been accounted for. Because of the modeling complication of a moving boundary problem, the deposit layer is usually assumed thin enough and does not affect flow fields. However, according to the field data from the Hassi Messaoud field [14], the South Kuwait's Marrat field [15], and the West Kuwait's Marrat field [16], the asphaltene deposit layer formed can block respectively about 44%, 60% and 55% of the cross-sectional area in these production strings. It is evident that the deposit layer is not thin and therefore should be considered. Modeling of the effect of growing deposit layer fully coupled with flow fields is present in Ge *et al.* [17]. In their model, no thermodynamic module was included, because particles are assumed carried by flow from the inlet and no precipitation occurs. In view of this, the present study intends to develop an integrated model for asphaltene deposition in wellbores/pipelines with the effect of growing deposit layer fully accounted for in a coupled manner to the flow and temperature fields and to the deposition process itself.

II. PROBLEM DESCRIPTION AND MODELING FRAMEWORK

In general, asphaltenes can exist in oil in different forms: dissolved asphaltene, precipitated asphaltene particle and aggregated asphaltene particle. Under reservoir condition (high p and high T), asphaltenes are stable in oil as dissolved asphaltenes. As oil flows up along the wellbore, both p and T drop continuously. When a specific p and T condition (i.e. asphaltene precipitation onset condition) is reached, asphaltene precipitation starts to occur forming small particles, i.e. precipitated asphaltene particles (Fig. 1). These small particles can agglomerate with each other to form aggregated asphaltene particles of a larger particle size (Fig. 1). The precipitated and aggregated asphaltene particles are transported (i) along the

flow direction from upstream to downstream, and (ii) along the radial direction from fluid bulk to near-wall region. In the present study, it is assumed that all aggregated asphaltene particles having larger inertia are carried by oil flow downstream, and only precipitated asphaltene particles can diffuse radial towards wall. Some of these precipitated asphaltene particles that reach the depositing front potentially stick to it and become deposits. This sticking process is asphaltene deposition. As more particles deposit over time, the asphaltene deposit layer grows gradually. Meanwhile, the fluid volume fraction decreases accompanied by an increase in both velocity (u) and pressure drop. The fluid volume fraction (α) in a given section of the wellbore/pipeline Δx is defined as

$$\alpha = \frac{V_f}{V_{CV}} = \frac{A_f \Delta x}{A \Delta x} = \frac{\pi r^2 \Delta x}{\pi R^2 \Delta x} = \frac{r^2}{R^2} \tag{1}$$

where A and A_f represent respectively cross-sectional area of the wellbore/pipeline and flow (Fig. 1c) with radii of R and r.

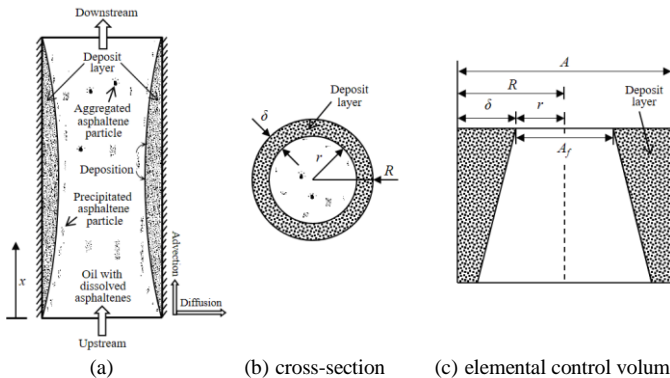(a)   (b) cross-section   (c) elemental control volume
Fig. 1. *Schematic of oil transportation in a circular wellbore/pipeline*

Based on the above description, a complete model of asphaltene deposition in wellbores/pipelines contains four ingredients: (i) asphaltene precipitation, (ii) fluid transport, (iii) particle transport, and (iv) asphaltene deposition. Among these, asphaltene precipitation predicts the amount of precipitated asphaltene particles formed at given p and T locally. Fluid transport predicts the flow fields (u and p) in the wellbore or pipeline. Particle transport predicts the distribution of various forms of asphaltenes (i.e. dissolved asphaltenes, precipitated asphaltene particles and aggregated asphaltene particles). Asphaltene deposition predicts the mass of precipitated asphaltene particles attaching onto the deposit front. These four ingredients interact with each other and are tightly coupled. Therefore, in order to give a more accurate prediction of all the physics involved, these four ingredients should be considered simultaneously. From a modeling point, these four ingredients can be grouped into two sub-modules: a Thermodynamic Module and a Transport Module.

III. MATHEMATICAL FORMULATION

A. Assumptions
- Only precipitated asphaltene particles can deposit.
- Rigid solid deposit with constant density.
- No shear removal of deposit.

- Oil density and viscosity depend only on p and T.
- Oil flow is single-phase multi-component fluid.

B. Transport Module
The governing equations are listed here.
Fluid transport

$$\frac{\partial}{\partial t}(\rho\alpha) + \frac{\partial}{\partial x}(\rho\alpha u) = -\dot{R}_{dep} \tag{2}$$

$$\frac{\partial}{\partial t}(\rho\alpha u) + \frac{\partial}{\partial x}(\rho\alpha uu) = -\alpha\frac{\partial p}{\partial x} + \rho\alpha g - f_w \tag{3}$$

$$\frac{\partial}{\partial t}(\rho c_p \alpha T) + \frac{\partial}{\partial x}(\rho c_p \alpha uT) = \dot{R}_T \tag{4}$$

Particle Transport

$$\frac{\partial}{\partial t}(\alpha C_{dis}) + \frac{\partial}{\partial x}(\alpha u C_{dis}) = -\dot{R}_{pre} \tag{5}$$

$$\frac{\partial}{\partial t}(\alpha C_{pre}) + \frac{\partial}{\partial x}(\alpha u C_{pre}) = \dot{R}_{pre} - \dot{R}_{dep} - \dot{R}_{agg} \tag{6}$$

Asphaltene deposition

$$\dot{R}_{dep} = \alpha k_{dep} C_{pre}^{m_{dep}} \tag{7}$$

$$\dot{R}_{dep} = \alpha k_{dep} C_{pre}^{m_{dep}} \tag{8}$$

$$\frac{d\alpha}{dt} = -\frac{\dot{R}_{dep}}{\rho_{dep}} \tag{9}$$

C. Thermodynamic Module
The rate of asphaltene precipitation ($\dot{R}_{pre}$) is given as [11]

$$\dot{R}_{pre} = \begin{cases} \alpha k_{pre}(C_{dis} - C_{eq}) & \text{,if } C_{dis} \geq C_{eq} \\ -\alpha k_{dis} C_{pre} & \text{,if } C_{dis} < C_{eq} \end{cases} \tag{10}$$

where C_{eq} is the equilibrium asphaltene concentration at the specified p and T. The oil of interest is assumed consisting of two liquid phases: an asphaltene lean liquid phase (L_1) and an asphaltene-rich liquid phase (L_2). All precipitated asphaltene particles exist only in L_2. C_{eq} is calculated by

$$C_{eq} = \rho_1 \cdot \frac{\beta_1 \upsilon_1}{\beta_1 \upsilon_1 + \beta_2 \upsilon_2} \cdot w_{asph\_L1} \tag{11}$$

where ρ, β, υ and w_{asph_L1} are respectively density, mole fraction, molar volume and weight fraction. A multi-component multi-phase flash calculation algorithm is developed based on the isothermal flash method of [19, 20] using the Peng-Robinson EOS [21, 22] with Peneloux volume translation [23] (PR-Peneloux EOS). The details of this flash calculation algorithm are presented in [18].

Liquid density (ρ_{liquid}) is calculated from

$$\rho_{liquid} = \frac{\beta_1 \sum_{i=1}^{N_c} x_i MW_i + \beta_2 \sum_{i=1}^{N_c} y_i MW_i}{\beta_1 \upsilon_1 + \beta_2 \upsilon_2} \tag{12}$$

and viscosity (μ_{liquid}) is determined based on the corresponding states viscosity model as introduced in [24].

IV. SOLUTION PROCEDURE
The governing equations, i.e. Eqs. (2-6), can be re-written in a general form:

$$\frac{\partial}{\partial t}\left(\tilde{\rho}\tilde{\phi}\right)+\frac{\partial}{\partial x}\left(\tilde{\rho}\tilde{\phi}u\right)=S_{\tilde{\phi}} \quad (13)$$

where $\tilde{\rho}$, $\tilde{\phi}$ and $S_{\tilde{\phi}}$ represent respectively the "appropriate" density, variable of interest and source term. Equation (13) is solved using the finite volume method [25, 26] on mesh shown in Fig. 2. The discretized general equation in the hatched control volume (CV) is

$$\left[\frac{\left(\tilde{\rho}\tilde{\phi}\right)_i^n-\left(\tilde{\rho}\tilde{\phi}\right)_i^{n-1}}{\Delta t}\right]\Delta V+\left[\left(\tilde{\rho}\tilde{\phi}u\right)_i^n-\left(\tilde{\rho}\tilde{\phi}u\right)_{i-1}^n\right]A$$
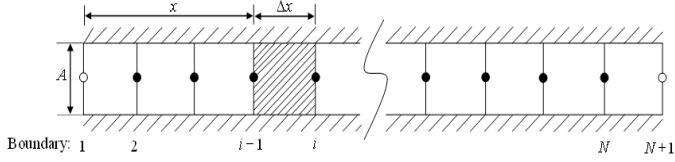$$=\left(S_{\tilde{\phi}}\right)_i^n\Delta V \quad (14)$$

Fig. 2. *Schematic representation of the discretized computational domain*

To integrate the two modules, a lookup table containing all the outputs of the Thermodynamic Module (i.e. C_{eq}, ρ_{liquid} and μ_{liquid}) is generated in advance for the oil of interest. During simulation, the Transport Module will linearly interpolate the required data from this table according to the predicted p and T.

V. RESULTS AND DISCUSSIONS

A. Verification and Validation of the Transport Module

The present Transport Module is employed to predict the experimental results of asphaltene deposition in capillary tube [12, 27]. In the simulation, $k_{pre} = 1.45\times10^{-3}$ s^{-1}, $k_{agg} = 5.07\times10^{-3}$ s^{-1} and $k_{dep} = 1.31\times10^{-2}$ s^{-1} determined in [12] are used. Besides, $C_{eq} = 0$ is set considering the fixed temperature condition and small pressure variation. Because of this setting, the Thermodynamic Module is not required. As for k_{dis}, due to the lack of information in existing studies, it is also set to zero.

Fig. 3a shows a much thicker deposit formed near the inlet and it becomes thinner downstream. This is because the precipitated asphaltene particle concentration near the inlet is higher, and it decreases along the capillary tube as deposition takes place resulting in a gradually lower potential to deposit. The deposit layer thickness at t=35.9h is compared to the experiment result of [12] in Fig. 3b. The prediction of the Transport Module agrees qualitatively with the measurement. By setting $C_{eq} = 0$ and $k_{dis} = 0$, the Transport Module overpredicts the amount of asphaltene deposit formed for x<17.2m. However, the measured deposit profile in the near-exit-region is not captured well by the Transport Module. The prediction shows almost minute asphaltene deposit is formed toward the outlet of the capillary tube owing to the exhaustion of precipitated asphaltene particle in the flowing oil-precipitant mixture. While the experiment result indicates a relatively high amount of deposit with an almost constant deposit thickness near the exit. This discrepancy may be caused by the use of constant kinetic parameters in the present model potentially insufficient to describe the processes

occurring in the entire capillary tube. In addition, the shear removal of upstream deposits and re-deposition downstream is also not accounted for in the present model. Nevertheless, the Transport Module is capable of predicting the overall trend of asphaltene deposit profile, in particular the location and magnitude of the maximum deposit layer thickness.
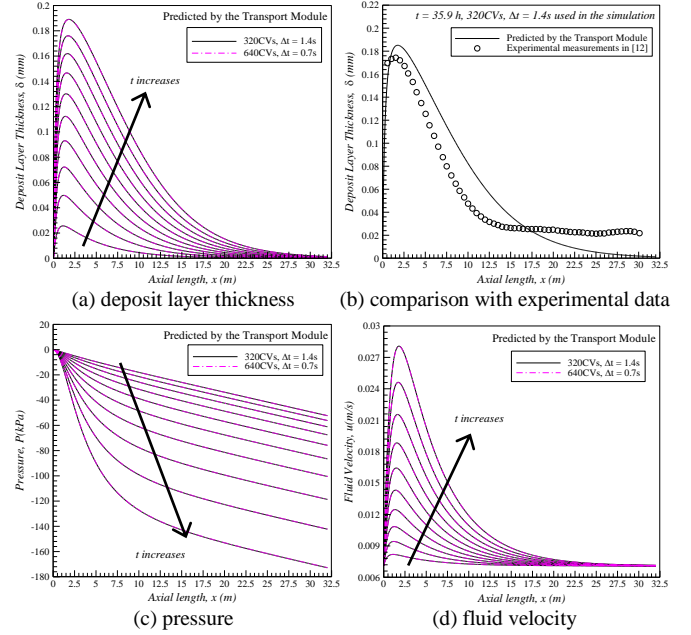

(a) deposit layer thickness   (b) comparison with experimental data

(c) pressure   (d) fluid velocity

Fig. 3. *Simulation results of the capillary asphaltene experiment*

B. Verification and Validation of the Thermodynamic Module

The Thermodynamic Module is used to predict w_{asph_L1} for one crude oil at varying pressures but a fixed temperature (322 K) and validate the prediction against the experiment data of [28]. The compositions of this oil in mol% are given in [30]. The asphaltene onset data and bubble points are extracted from [29]. The relevant parameters of this oil after characterization and the binary interaction parameters (BIPs) employed in simulation are presented in [18].

Fig. 4a shows the comparison between the predicted asphaltene precipitation envelope (APE) and the available asphaltene onset data and bubble pressures (BP) for Oil 1. The Thermodynamic Module under-predicts BP slightly with an average discrepancy of 10.25%, but gives accurate predictions of the upper asphaltene onset pressure (UAOP) and lower asphaltene onset pressure (LAOP). Besides, the predicted oil density is 39.83°API, which matches the range of 36°–40°API reported in [29]. In addition, the prediction of the asphaltene content in stock tank oil (STO) is 0.545 wt%. This agrees very well with the experimental value of 0.5 wt% C_7-asphaltene through SARA analysis in [29].

The predicted w_{asph_L1} by the Thermodynamic Module is compared with available experiment data in Fig. 4b. w_{asph_L1} drops almost linearly in the 'L$_1$+L$_2$' region, and the prediction is consistent with the experimental data in [28]. However, although the trends are similar, the predicted w_{asph_L1} in the 'L$_1$+L$_2$+V' region deviates from the experimental measurements. This may arise from the poor prediction of BP.

Overall, the Thermodynamic Module is able to give a reasonably accurate prediction of w_{asph_L1} in accordance with the asphaltene phase behaviors at varying pressures but fixed temperature (322K). This case verifies and validates the Thermodynamic Module.
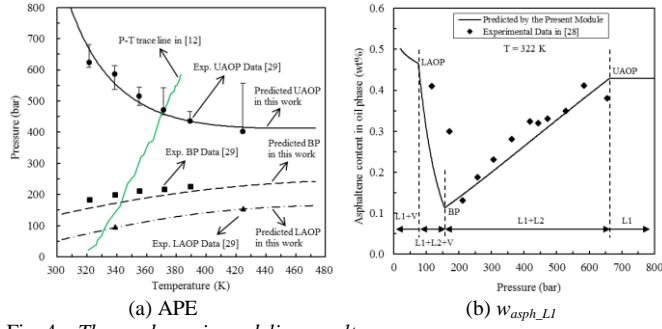

<center>(a) APE   (b) w_{asph_L1}</center>

Fig. 4. *Thermodynamic modeling results*

C. Case Study: Field Asphaltene Deposition Problem

The model is applied for asphaltene deposition problem in South Kuwait's Marrat field [15]. The depth, diameter and oil production rate are respectively 15000ft, 2.75in and 5000STB/day. Besides, $k_{pre} = 1.8 \times 10^{-3}$ s^{-1}, $k_{dis} = 1.7 \times 10^{-2}$ s^{-1}, $k_{agg} = 1.8 \times 10^{-3}$ s^{-1}, and $k_{dep} = 2.1 \times 10^{-4}$ s^{-1} are used.

The crude oil sample from the same well was studied thermodynamically in previous section (Fig. 4). The predicted APE (Fig. 4a) together with the operating conditions given in [12]. The operating conditions in the same wellbore are indicated by a P-T trace line, from which the p and T at reservoir are found as 8497psia and 230°F, and those at wellhead are 321psia and 118°F (Fig. 4a). The operating conditions span all those regions divided by the APE. However, the current Transport Module is limited only for single-phase or homogenous flow. It cannot be used when p and T are below bubble point where one more vapor phase is formed in oil. Similar to the work done in [12], the average velocity (2.40m/s) is prescribed throughout the entire wellbore. Besides, both of p and T are assumed to vary linearly from reservoir to wellhead. Under these assumptions, the conservation equations of fluid mass, momentum and energy are not solved during simulation. Only α, C_{dis} and C_{pre} require to be determined.

Finally, the predicted δ, C_{dis} and C_{pre} by the developed model are presented in Fig. 5. From Fig. 5a, asphaltene deposition occurs at around 12000-ft well depth and then strengthens continuously till its peak at approximately 4000-ft. After that, asphaltene deposition decreases rapidly and almost diminishes at the location of 1500-ft well depth. This can be explained by the variation of asphaltene concentration. Shown in Fig. 5b, above UAOP, the predicted C_{dis} is slightly larger than C_{eq}. This is because both of p and T in the wellbore deplete when oil flows up leading to a small decrease of C_{eq}. However, the difference between C_{dis} and C_{eq} is so small that the extent of asphaltene precipitation is negligible. Below UAOP, asphaltene precipitation occurs and C_{eq} decreases dramatically. The larger difference between C_{dis} and C_{eq} stands for stronger asphaltene precipitation. The predicted C_{pre}

increases continuously from UAOP to BP (Fig. 5c). When the operating condition falls below BP, some light components come out making the oil more stable. In this instance, C_{eq} increases. Nevertheless, at this moment, C_{dis} is still larger than C_{eq}, which implies that asphaltene precipitation continues consuming dissolved asphaltenes. When C_{dis} is lower than C_{eq}, the re-dissolution of precipitated asphaltene particles happens. Consequently, C_{dis} increases slightly. Meanwhile, the re-dissolution process exhausts precipitated asphaltene particles, therefore asphaltene deposition alleviates and finally ceases.

In Fig. 6, the deposit layer thickness predicted by the model is compared with simulation result of [12] and caliper measurements in [31]. Fig. 6a shows that the present model gives a similar prediction of asphaltene deposit profile but shifted downstream (towards the wellhead). The prediction of the maximum deposit layer thickness locates at the well depth of almost 2800-ft, whereas in [12] it is around 4200-ft. This is because, as discussed in the former section, the Thermodynamic Module under-predicts the BP about 10.25% on average. However, asphaltene deposition reaches its peak just at BP as shown in Fig. 5a. As p decreases continuously during oil transportation, the under-prediction of BP leads to the shift of the maximum deposit point downstream in the wellbore. The inaccuracy of BP prediction may stem from the parameter acquisition process where the required parameters are only tuned to match available UAOP data rather than BP data. In Fig. 6b, the predicted deposit layer thickness is translated 1500-ft upstream to account for the under-prediction of BP. The predicted deposit profile is consistent with the measurements in [31]. Therefore, provided that a more accurate prediction of BP is available, the present model is able to give a reasonably accurate prediction of asphaltene deposition profile.
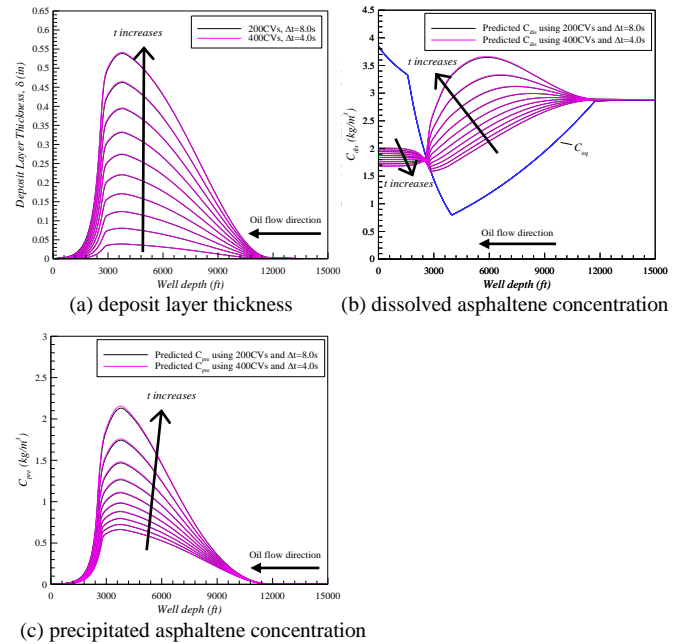

<center>(a) deposit layer thickness   (b) dissolved asphaltene concentration</center>

<center>(c) precipitated asphaltene concentration</center>

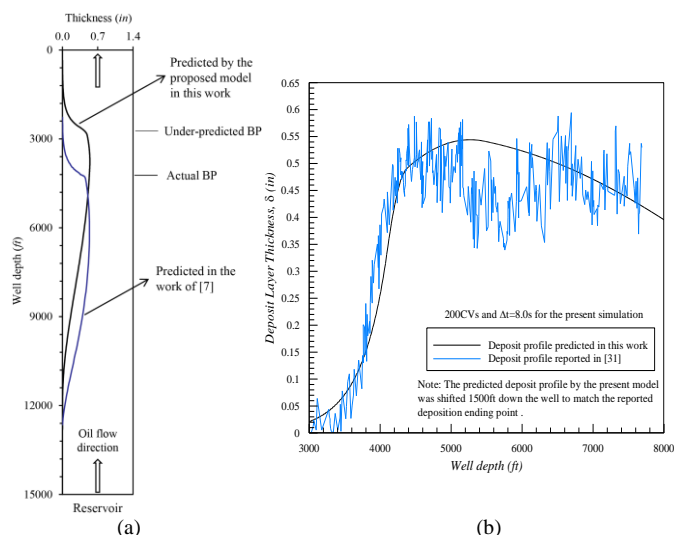Fig. 5. *Thermodynamic modeling results*

Fig. 6. *Prediction of asphaltene deposit layer thickness by the model compared with the simulation results of [12] (a) and the experimental measurements of [31] (b).*

VI. CONCLUSIONS AND RECOMMENDATIONS

A one-dimensional asphaltene deposition model in wellbores/pipelines is presented. This model considers the processes involved simultaneously through integrating the Thermodynamic Module with the Transport Module. Those two modules are first verified and validated separately. Then it is used to investigate an oil field asphaltene deposition problem. The model gives a reasonably accurate prediction of asphaltene deposit layer profile. The model accounts for the variation in the flow cross-sectional area due to the deposit layer. This variation affects u and p fields and eventually asphaltene precipitation and deposition. As for the next task, two-phase flow model needs to be incorporated together with a more accurate EOS (e.g. PC-SAFT EOS).

REFERENCES

[1] K. Akbarzadeh, A. Hammami, A. Kharrat, D. Zhang, S. Allenson, J. Creek, et al., "Asphaltenes—Problematic but Rich in Potential," Oilfield Review, vol. 19, pp. 22-43, 2007.

[2] G. A. Mansoori, "Remediation of Asphaltene and Other Heavy Organic Deposits in Oil Wells and in Pipelines," SOCAR Proceedings, vol. 2010, pp. 12-23, 2010.

[3] M. P. Hoepfner, V. Limsakoune, V. Chuenmeechao, T. Maqbool, and H. S. Fogler, "A Fundamental Study of Asphaltene Deposition," Energy & Fuels, vol. 27, pp. 725-735, 2013.

[4] J. L. Creek, "Freedom of Action in the State of Asphaltenes: Escape from Conventional Wisdom," Energy & Fuels, vol. 19, pp. 1212-1224, 2005.

[5] E. Ramirez-Jaramillo, C. Lira-Galeana, and O. Manero, "Modeling Asphaltene Deposition in Production Pipelines," Energy & Fuels, vol. 20, pp. 1184-1196, 2006.

[6] B. S. Soulgani, D. Rashtchian, B. Tohidi, and M. Jamialahmadi, "Integrated Modelling Methods for Asphaltene Deposition in Wellstring," Journal of the Japan Petroleum Institute, vol. 52, pp. 322-331, 2009.

[7] D. H. Beggs and J. P. Brill, "A Study of Two-Phase Flow in Inclined Pipes," Journal of Petroleum technology, vol. 25, pp. 607-617, 1973.

[8] A. Hirschberg, L. DeJong, B. Schipper, and J. Meijer, "Influence of Temperature and Pressure on Asphaltene Flocculation," Society of Petroleum Engineers Journal, vol. 24, pp. 283-293, 1984.

[9] D. Eskin, J. Ratulowski, K. Akbarzadeh, and S. Pan, "Modelling Asphaltene Deposition in Turbulent Pipeline Flows," The Canadian Journal of Chemical Engineering, vol. 89, pp. 421-441, 2011.

[10] K. Akbarzadeh, D. Eskin, J. Ratulowski, and S. Taylor, "Asphaltene Deposition Measurement and Modeling for Flow Assurance of Tubings and Flow Lines," Energy & Fuels, vol. 26, pp. 495-510, 2011.

[11] F. M. Vargas, J. L. Creek, and W. G. Chapman, "On the Development of an Asphaltene Deposition Simulator," Energy & Fuels, vol. 24, pp. 2294-2299, 2010.

[12] A. S. Kurup, F. M. Vargas, J. Wang, J. Buckley, J. L. Creek, H. Subramani, J, et al., "Development and Application of an Asphaltene Deposition Tool (ADEPT) for Well Bores," Energy & Fuels, vol. 25, pp. 4506-4516, 2011.

[13] A. S. Kurup, J. Wang, H. J. Subramani, J. Buckley, J. L. Creek, and W. G. Chapman, "Revisiting Asphaltene Deposition Tool (ADEPT): Field Application," Energy & Fuels, vol. 26, pp. 5702-5710, 2012.

[14] C. E. Haskett and M. Tartera, "A Practical Solution to the Problem of Asphaltene Deposits-Hassi Messaoud Field, Algeria," Journal of Petroleum Technology, vol. 17, pp. 387-391, 1965.

[15] C. Kabir, A. Hasan, D. Lin, and X. Wang, "An Approach to Mitigating Wellbore Solids Deposition," in SPE Annual Technical Conference and Exhibition, 2001.

[16] S. F. Alkafeef, F. Al-Medhadi, and A. D. Al-Shammari, "A Simplified Method to Predict and Prevent Asphaltene Deposition in Oilwell Tubings: Field Case," in SPE Annual Technical Conference and Exhibition, 2003.

[17] Q. Ge, Y. Yap, F. Vargas, M. Zhang, and J. Chai, "Numerical Modeling of Asphaltene Deposition," Computational Thermal Sciences, vol. 5, pp. 153-163, 2013.

[18] Q. Guan, "Asphaltene Deposition in One Dimensional Multicomponent Flows," Master of Science, The Petroleum Institute (United Arab Emirates), 2016.

[19] M. L. Michelsen, "The Isothermal Flash Problem. Part I. Stability," Fluid Phase Equilibria, vol. 9, pp. 1-19, 1982.

[20] M. L. Michelsen, "The Isothermal Flash Problem. Part II. Phase-Split Calculation," Fluid Phase Equilibria, vol. 9, pp. 21-40, 1982.

[21] D.-Y. Peng and D. B. Robinson, "A New Two-Constant Equation of State," Industrial & Engineering Chemistry Fundamentals, vol. 15, pp. 59-64, 1976.

[22] D. B. Robinson and D.-Y. Peng, The Characterization of the Heptanes and Heavier Fractions for the GPA Peng-Robinson Programs: Gas Processors Association, 1978.

[23] A. Péneloux, E. Rauzy, and R. Fréze, "A Consistent Correction for Redlich-Kwong-Soave Volumes," Fluid Phase Equilibria, vol. 8, pp. 7-23, 1982.

[24] K. S. Pedersen, P. L. Christensen, and J. A. Shaikh, Phase Behavior of Petroleum Reservoir Fluids: CRC Press, 2006.

[25] S. V. Patankar, Numerical Heat Transfer and Fluid Flow. New York: Hemisphere Publisher, 1980.

[26] H. K. Versteeg and W. Malalasekera, An Introduction to Computational Fluid Dynamics: The Finite Volume Method, 2nd ed. England: Prentice Education Limited, 2007.

[27] J. Wang, J. S. Buckley, and J. L. Creek, "Asphaltene Deposition on Metallic Surfaces," Journal of Dispersion Science and Technology, vol. 25, pp. 287-298, 2004.

[28] X. Zhang, N. Pedrosa, and T. Moorwood, "Modeling Asphaltene Phase Behavior: Comparison of Methods for Flow Assurance Studies," Energy & Fuels, vol. 26, pp. 2611-2620, 2012.

[29] C. Kabir and A. Jamaluddin, "Asphaltene Characterization and Mitigation in South Kuwait's Marrat Reservoir," in Middle East Oil Show and Conference, 1999.

[30] A. Arya, N. von Solms, and G. M. Kontogeorgis, "Determination of Asphaltene Onset Conditions Using the Cubic Plus Association Equation of State," Fluid Phase Equilibria, vol. 400, pp. 8-19, 2015.

[31] C. Kabir and A. Jamaluddin, "Asphaltene Characterization and Mitigation in South Kuwait's Marrat Reservoir," SPE Production & Facilities, vol. 17, pp. 251-258, 2002.